



# Cyclooxygenase-2 mediates puerarin to inhibit the invasion and metastasis of lung cancer A549 cells

Yun Zeng<sup>1,2</sup>, Zheng-Jie Shen<sup>1</sup>, Wen-Zhe Gu<sup>3</sup>, Mian-Hua Wu<sup>1</sup>

<sup>1</sup>First Clinical College, Nanjing University of Chinese Medicine, Nanjing 210023, China; <sup>2</sup>Department of Medical Oncology, Jiangsu Cancer Hospital, Nanjing 210009, China; <sup>3</sup>Department of Otorhinolaryngology, Zhangjiagang Hospital of Traditional Chinese Medicine, Zhangjiagang 215600, China

**Contributions:** (I) Conception and design: Y Zeng; (II) Administrative support: Y Zeng; (III) Provision of study materials or patients: Y Zeng; (IV) Collection and assembly of data: ZJ Shen, WZ Gu, MH Wu; (V) Data analysis and interpretation: ZJ Shen, WZ Gu, MH Wu; (VI) Manuscript writing: All authors; (VII) Final approval of manuscript: All authors.

**Correspondence to:** Mian-Hua Wu. First Clinical College, Nanjing University of Chinese Medicine, Nanjing 210023, China.

Email: wumianhuafcc@hotmail.com.

**Background:** The mechanisms by which puerarin prevents and treats lung cancer remain largely unknown. We aimed to study the roles of puerarin in the invasion and metastasis of lung cancer A549 cells based on cyclooxygenase-2 (COX-2).

**Methods:** The effects of different concentrations of puerarin on the proliferation of A549 cells were evaluated. The *in vitro* and *in vivo* effects of puerarin on the invasion and metastasis of A549 cells were assessed by Transwell assay and an animal model of tumor lung metastasis respectively. The influence of puerarin on COX-2 in A549 cells was also analyzed in terms of enzymatic activity and tissue level to explore the role of COX-2 in the inhibitory effects of puerarin on cell invasion and metastasis.

**Results:** Puerarin inhibited the proliferation of A549 cells in time- and dose-dependent manners. Compared with the control group, more cells in the puerarin treatment groups were arrested in the G0/G1 phase, but the proportion of S phase cells decreased. Puerarin blocked the cell cycle dose-dependently. After 24 h of culture with 200 µg/mL puerarin, significantly fewer cells penetrated the basement membrane of Transwell chambers than those in the control group, and the MMP-2/TIMP-2 levels in PUE200, PUE400 and PUE800 groups significantly dropped. For the animal experiments, the puerarin treatment groups had significantly fewer and smaller tumors with pulmonary metastasis than those of the control group. After 24 h of culture with puerarin, like the indomethacin (IN) group, PUE200, PUE400 and PUE800 groups had significantly lower enzymatic activity of COX-2 than that of the control group, but the puerarin treatment groups had similar results. The IN group had lower COX-2 protein expression than that of the control group, but the puerarin treatment groups had similar expressions to that of the control group, indicating that COX-2 protein expression was hardly affected by puerarin in A549 cells. Similar to the IN group, the puerarin treatment groups had significantly lower PGE2 levels than that of the control group ( $P < 0.05$ ). However, there was no significant difference between PUE200, PUE400 and PUE800 groups. The tumors with pulmonary metastasis from the puerarin treatment groups had significantly lighter colors of COX-2 positive cells and particles than those of the control group.

**Conclusions:** Puerarin inhibited the enzymatic activity of COX-2 in A549 cells and its expression in tumor tissues with pulmonary metastasis. MMP-2/TIMP-2 may be one of the mechanisms by which puerarin inhibits the invasion of A549 cells.

**Keywords:** Lung cancer; puerarin; cyclooxygenase-2 (COX-2); invasion; metastasis

Submitted Feb 14, 2017. Accepted for publication Apr 21, 2017.

doi: 10.21037/tcr.2017.06.18

**View this article at:** <http://dx.doi.org/10.21037/tcr.2017.06.18>

## Introduction

The mortality rate of patients with lung cancer ranks first among all cancers worldwide, severely endangering human health (1). Chemotherapy and radiotherapy, which are often accompanied by serious toxic side reactions, cannot fundamentally change this situation. At present, the 5-year survival rate of lung cancer is still as low as 10% (2), so it is urgent to find new, effective treatment strategies. Compared with traditional drugs for chemotherapy, targeted antitumor agents affect the overexpression or mutation in tumor cells and molecules closely associated with malignant biological behaviors instead of directly killing the cells, thereby suppressing excessive proliferation, angiogenesis, invasion and metastasis (3,4). Gefitinib and erlotinib have been clinically applied to treat non-small cell lung carcinoma (NSCLC) targeting epidermal growth factor receptors (5). Although the therapeutic effects of targeted antitumor agents still need further observation, this strategy has indeed benefited patients with lung cancer, with fewer toxic side reactions and better compliance. Researchers have endeavored to find new targets for preventing and treating tumors.

Cyclooxygenases (COXs) are key rate-limiting enzymes that decompose arachidonic acid into various endogenous prostaglandins (PGs) (6). Of the two COXs COX-1 and COX-2 (7), the latter plays important roles in inflammatory response, being closely related with the onset, metastasis and prognosis of lung cancer (8-10). COX-2 is highly expressed in approximately 70% of lung cancer tissues, and expressed in about 1/3 of atypical adenoma and carcinoma *in situ* (11). In metastatic lymph nodes, the number of COX-2 positive cells exceeds that in primary tumors (12). By using *in situ* hybridization, Paleari *et al.* found in 160 samples of patients with Stage I NSCLC that the survival times of highly COX-2 positive, moderately to mildly positive and no COX-2 expression groups were 1.04, 5.50 and 8.54 years respectively (13), with significant differences. Therefore, the survival time of patients with early NSCLC in whom COX-2 was positively expressed was shortened. COX-2 has the highest and widest expression in adenocarcinoma of NSCLC, followed by squamous cell carcinoma. In contrast, moderate COX-2 expression is occasionally detected in cases with small cell lung carcinoma. Besides, it is not or only mildly expressed in normal bronchial epithelial cells and alveolar epithelial cells (14). COX-2 affects tumor invasion and metastasis via diverse mechanisms, including mediation of increase in

CD44 (cell surface hyaluronic acid receptor) expression to promote tumor cell adhesion (15), induction of production of metalloprotease 2 that degrades extracellular matrix to open the pathway for cell invasion and metastasis, and induction of deletion of E-cadherin to facilitate tumor cell metastasis through detachment from the primary lesion.

Puerarin, as an isoflavone extracted from the dried root of traditional Chinese medicine plant *Pueraria lobata*, has high antioxidative capacity (16). In addition, it has well-documented antitumor activities (17,18), but the detailed mechanisms remain unclear. To this end, we explored the roles of puerarin in lung cancer invasion and metastasis based on COX-2. According to the expression characteristics of COX-2 in lung cancer, we selected human A549 cells. Up to now, the influence of puerarin on A549 cells has seldom been reported. In this study, the effects of puerarin on their proliferation were evaluated. The *in vitro* and *in vivo* effects of puerarin on the invasion and metastasis of A549 cells were assessed by Transwell assay and an animal model of lung metastasis respectively. The influence of puerarin was also studied in terms of the enzymatic activity, protein expression, metabolites and tissue level of COX-2. Meanwhile, a non-selective COX inhibitor indomethacin (IN), which has been verified to inhibit the activity and protein expression of COX-2 in NSCLC, was selected as the positive control drug (19). The results may provide valuable evidence for clarifying the signaling pathways in lung cancer invasion and metastasis, and a potentially eligible antitumor agent targeting COX-2.

## Methods

### Cell culture

Human lung cancer cell line A549 (Institute of Radiation Medicine, Academy of Military Medical Sciences, Beijing, China) was cultured in DMEM containing 10% fetal bovine serum (FBS) (Hyclone, Logan, UT, USA) in a 37 °C incubator with 95% O<sub>2</sub> and 5% CO<sub>2</sub>.

### Flow cytometry

A549 cells in the logarithmic growth phase were routinely digested, inoculated into 6-well plates (approximately 1×10<sup>6</sup>/well), and cultured in a 37 °C incubator with 5% CO<sub>2</sub>. DMEM containing puerarin (Sinopharm Chemical Reagent Beijing Co., Ltd., Beijing, China) or IN (Sinopharm Chemical Reagent Beijing Co., Ltd.) was added 8 h

later, and the cells were divided into a control group, a 200 µg/mL puerarin group, a 400 µg/mL puerarin group, an 800 µg/mL puerarin group and a positive control 200 pM IN group. The final volume of each well was 2 mL. Then the cells were further incubated in the 37 °C incubator with 5% CO<sub>2</sub> for 24, 48 and 72 h respectively. After culture, the cells were routinely cultured, collected into 10 mL centrifuge tubes, and centrifuged at 500 ×g for 2 min, from which the supernatant was discarded. The cells were then washed and centrifuged again at 500 ×g for 2 min, from which the supernatant was discarded. Subsequently, the procedure was repeated, and 100 µmol/mL propidium iodide (Sigma Aldrich, St. Louis, MO, USA) was added and reacted in dark at 4 °C for 1 h. Cell DNA content was detected by flow cytometer (BD Pharmingen, San Diego, CA, USA), and the cell number in each phase of cell cycle was analyzed by FlowJo (BD Pharmingen, San Diego, CA, USA). The experiment for each group was conducted at least three times.

#### *Transwell assay (20)*

A549 cells in the exponential growth phase were cultured in serum-free DMEM, and cultured in a 37 °C incubator with 5% CO<sub>2</sub> for 24 h. Afterwards the cells were routinely digested and resuspended in DMEM containing 1% BSA. Then the cell concentration was adjusted and added into Matrigel-coated Transwell chambers, 4×10<sup>4</sup> cells/chamber. The chambers were thereafter placed into a 24-well plate, with DMEM containing 10% FBS added into each well outside the chambers. After 6 h of culture in the 37 °C incubator with 5% CO<sub>2</sub>, the cells were divided into a 200 µg/mL puerarin group and a control group. The final volume of each Transwell chamber (Corning, New York, USA) was 200 µL. Six replicate wells were set for each group. After another 24 h of culture, the chambers were taken out, and the cells therein were wiped off by a cotton swab. Finally, the chambers were washed four times with PBS, fixed in absolute methanol for 20 min, and stained by 0.2% crystal violet (Gemini Bio-Products, Woodland, CA, USA) for 30 min. Five visual fields were randomly selected to count the cells and to calculate the mean. The above experiments were repeated at least five times.

#### *ELISA*

A549 cells in the exponential growth phase were cultured in serum-free DMEM, inoculated into 24-well plates and

divided into a control group, a 200 µg/mL puerarin group, a 400 µg/mL puerarin group, an 800 µg/mL puerarin group and a positive control 200 pM IN group. They were then cultured in a 37 °C incubator with 5% CO<sub>2</sub> for 24 h, and the supernatant was collected into EP tubes and stored at -80 °C before use. A standard curve was plotted. In seven wells, the sample was diluted into the final concentrations of 8,000, 4,000, 2,000, 1,000, 500, 250 and 125 pg/mL respectively (100 µL/well). The eighth well was blank control. Then 100 µL/well culture supernatant was added. The plate (R&D Systems, Wiesbaden, Germany) was mixed thoroughly, sealed and incubated at room temperature for 2 h. Afterwards, the liquid was discarded, and the plate was washed three times and pat-dried. The working solution of primary antibody (100 µL) was added into each well, and the plate was well mixed, sealed and incubated for 2 h at room temperature. Then the liquid was discarded, and the plate was washed three times and pat-dried. The working solution of HRP-labeled antibody (100 µL) was added into each well before another 20 min of incubation at room temperature in dark. After the liquid was discarded, the plate was washed three times and pat-dried. Then 100 µL of color development solution was added into each well and incubated for 20 min in dark at room temperature. After 50 µL of stopping solution NH<sub>2</sub>SO<sub>4</sub> was added into each well, the optical density at 450 nm was immediately detected by microplate reader (Thermo Scientific, Waltham, MA, USA) and corrected by that at 570 nm. The above experiments were repeated at least three times.

#### *Animal experiments (21)*

Healthy SPF male Balb/c nude mice aged 6 weeks and weighing 20–25 g were provided by Shanghai Laboratory Animal Center, CAS, China. All experiments were performed in accordance with the guidelines for the care and use of laboratory animals and related ethical regulations of Jiangsu Cancer Hospital. A549 cells in the exponential growth phase were routinely digested, washed twice with PBS, filtered by a 200-mesh sieve into single ones, resuspended in serum-free DMEM and adjusted to the concentration of 1×10<sup>7</sup>/mL. The tails of eight nude mice were immersed in 45 °C water for 2 min to dilate the tail vein into which the single suspension of A549 cells was injected through a 1 mL syringe (2×10<sup>6</sup>/0.2 mL each mouse), with the needle hole clamped for 2 min. Eight mice were weighed on the second day after inoculation and randomly divided into a PUE group and a control group (n=4).

The PUE group was intraperitoneally given 100 mg/kg/d puerarin and the control group was given the same volume of normal saline from the second day after injection of A549 cells. The mice were killed by cervical dislocation 28 days later, from which bilateral lungs were collected on ice. The pulmonary metastasis was observed by the naked eye and under a microscope to determine the optimum time for further experiments. Finally, the lungs were stored in 4% formaldehyde solution.

### *HE staining*

The paraffin sections of mouse lung tissues were routinely deparaffinized, hydrated, stained in hematoxylin (Sinopharm Chemical Reagent Beijing Co., Ltd.) for 2–3 min, rinsed continuously by water for 30 min, stained in eosin-ethanol solution (Sinopharm Chemical Reagent Beijing Co., Ltd.) for 1–2 min, dehydrated in 95% ethanol for 10 min and in 100% ethanol for 10 min, transparentized by xylene, mounted by neutral mounting medium, and observed under a microscope (Olympus, Tokyo, Japan).

### *Immunohistochemical assay*

Lung tissues of mice bearing metastatic tumors were fixed in 4% formaldehyde solution. The paraffin sections were deparaffinized by xylene (10 min, 3 times), dehydrated by series of ethanol solutions, placed in 10 mM citrate buffer (pH 6.0) (Sigma Aldrich, St. Louis, MO, USA), and heated in a microwave oven for 10 min to keep the temperature at 98 °C. Subsequently, they were taken out, cooled to room temperature, washed with PBS (5 min, 3 times), and incubated in 3% hydrogen peroxide/methanol at room temperature for 10 min to eliminate the activity of endogenous peroxidase. Then the sections were washed by PBS (5 min, 3 times), added a drop of goat serum for blocking after excess liquid was blotted, and incubated in a 37 °C humidified box for 10 min. After excess liquid was blotted, mouse anti-human monoclonal COX-2 antibody (Abcam, Cambridge, UK) (1:100 dilution by PBS containing 1% BSA and 0.05% Tween 20) was added into each section, incubated at 4 °C overnight, washed by PBS (5 min, 3 times), incubated with anti-mouse biotinylated secondary antibody at 37 °C for 30 min, washed by PBS (5 min, 3 times), then incubated with HRP-labeled streptavidin at 37 °C for 10 min, and washed with PBS (5 min, 3 times). The sections were thereafter color-developed by DAB solution (Boster

Biological Technology Co., Ltd., Wuhan, China), observed under a microscope until brownish yellow particles appeared, washed thoroughly with tap water, counterstained by hematoxylin, dehydrated with series of ethanol solutions, transparentized by xylene, mounted by neutral mounting medium, and observed under a microscope (Olympus, Tokyo, Japan). The brownish yellow or brown particles located by antigen were determined as positive.

### *Detection of COX-2 protein expression by Western blot*

Cells were collected, from which total protein was extracted. The protein was subjected to SDS-PAGE after the concentration was measured with the BCA method, electronically transferred to a nitrocellulose membrane at 120 mA and 4 °C for 2.5–3 h, and detected by Ponceau staining. After destaining in distilled water, the membrane was washed three times with TBST, blocked in TBST +5% skimmed milk at room temperature for 1 h, incubated overnight with anti-COX-1 (diluted by 1:300), anti-COX-2 (diluted by 1:500) and anti- $\beta$ -actin (diluted by 1:1,000) antibodies at 4 °C, washed four times with TBST, incubated with HRP-labeled secondary antibody (diluted by 1:3,000) at room temperature for 1 h, washed four times again with TBST and finally developed with ECL reagent for observation.

### *Statistical analysis*

All data were expressed as mean  $\pm$  standard error of measurement and analyzed by SPSS19.0 (SPSS Inc., Chicago, USA). Inter-group comparisons were performed by one-way analysis of variance followed by Dunnett's test.  $P < 0.05$  was considered statistically significant.

## **Results**

### *Effects of puerarin on the viability of A549 cells*

After treatment with puerarin for 24 h, 48 h and 72 h, MTT assay showed that the growth's inhibition rate increased with rising dose and extended time (*Figure 1*).

### *Effects of puerarin on the proliferation and cycle of A549 cells*

Puerarin inhibited the proliferation of A549 cells in time-

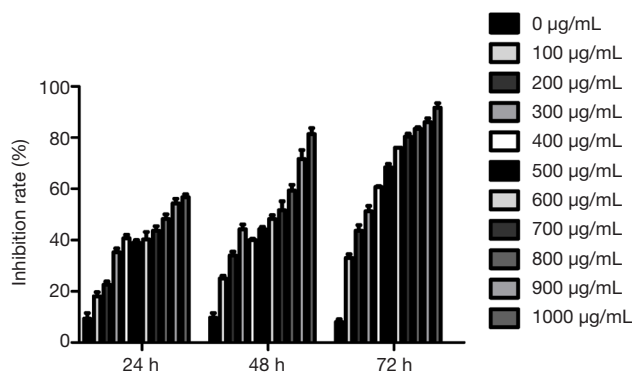


**Figure 1** Effects of puerarin on the viability of A549 cells.

and dose-dependent manners (*Figure 2A*). Since the survival rate of A549 cells first decreased sharply with increasing dose of puerarin to 400 µg/mL and then gradually leveled off, this dose was optimum for inhibiting the proliferative activity. Flow cytometry showed that compared with the control group, more cells in the puerarin treatment groups were arrested in the G0/G1 phase (*Figure 2B*), but the proportion of S phase cells decreased (*Figure 2C*). Puerarin blocked the cell cycle dose-dependently.

#### Effects of puerarin on the invasion of A549 cells

After 24 h of culture with 200 µg/mL puerarin, significantly fewer cells penetrated the basement membrane of Transwell chambers than those in the control group ( $P < 0.05$ ), indicating that puerarin significantly suppressed the invasion of A549 cells (*Figure 3A,B*). Besides, the MMP-2/TIMP-2 levels in the supernatants of A549 cells were detected by ELISA after puerarin treatment. After 24 h of culture, the levels in PUE200, PUE400 and PUE800 groups significantly dropped compared those of the control group, suggesting that the secretion of MMP-2/TIMP-2 was inhibited by puerarin. The inhibitory effect was enhanced with increasing puerarin dose, and the MMP-2/TIMP-2 levels of the PUE800 group were similar to those of the 200 µM IN group (*Figure 3C*).

#### Effects of puerarin on the distal metastasis of A549 cells

A mouse model of lung metastasis was established by injection of A549 cells via the tail vein to evaluate the influence of puerarin on *in vivo* distal metastasis. After successful modeling, there were obvious semitransparent

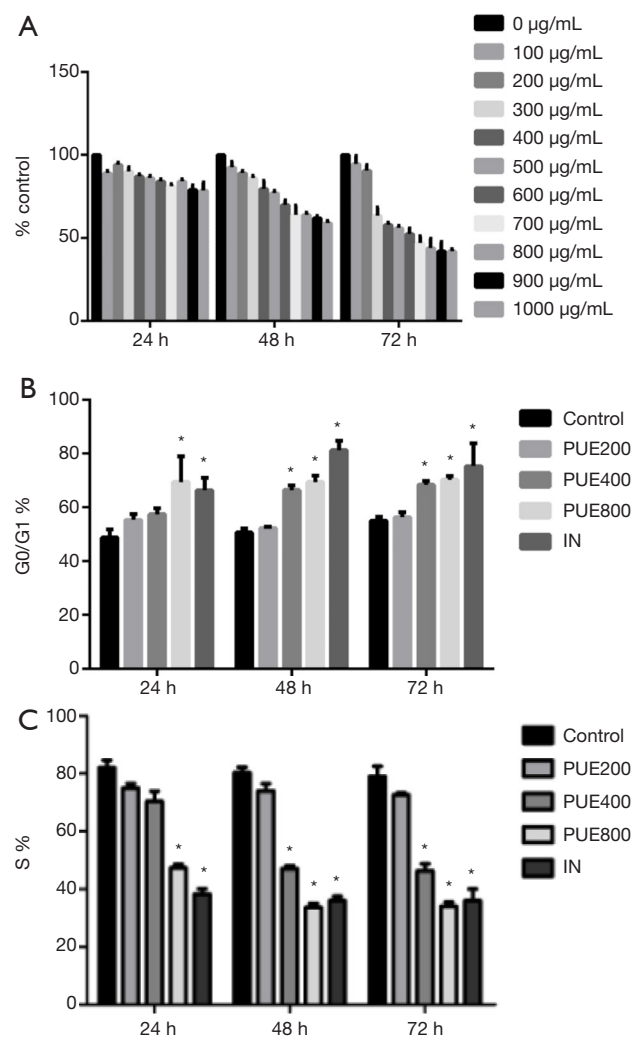


**Figure 2** Effects of puerarin on the proliferation (A) and cycle (B,C) of A549 cells. \*,  $P < 0.05$ , compared with the control group.

small-nodular metastatic tumors on the lung surface and in the lung parenchyma, which were spherical- or oval-shaped without uniform sizes (*Figure 4A*). A large number of metastatic foci appeared on the lung surface on the 40th day after inoculation, and the lung texture was rather hard. Meanwhile, the mice suffered from polypnea, poor appetite and decreased activity. After intraperitoneal injection of 100 mg/kg/day puerarin for 28 days, the number of metastatic tumors significantly decreased compared with that of the control group ( $P < 0.05$ ) (*Figure 4B*). HE staining showed that the puerarin treatment groups had significantly fewer and smaller tumors with pulmonary metastasis than those of the control group (*Figure 4C*).



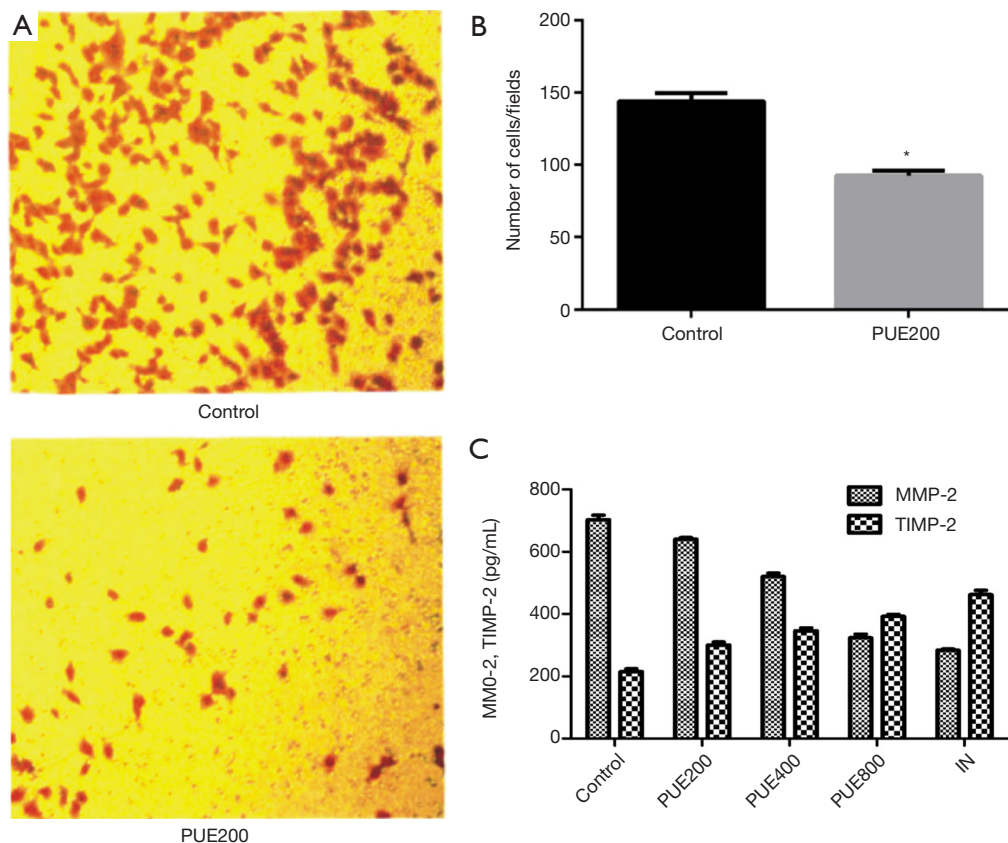


**Figure 3** Effects of puerarin the invasion of A549 cells. (A,B) Transwell assay results ( $\times 200$ ); (C) ELISA results of MMP-2/TIMP-2 levels in the supernatants of A549 cells after puerarin treatment. \*,  $P < 0.05$ , compared with the control group.

#### Effects of puerarin on the enzymatic activity of COX-2 and PGE2

After 24 h of culture with puerarin, like the IN group, PUE200, PUE400 and PUE800 groups had significantly lower enzymatic activity of COX-2 than that of the control groups, but the puerarin treatment groups had similar results (Figure 5A). Similar to the IN group, the puerarin treatment groups had significantly lower PGE2 levels in the supernatants than that of the control group ( $P < 0.05$ ). However, there was no significant difference between PUE200, PUE400 and PUE800 groups (Figure 5B). Immunohistochemical assay exhibited that COX-2 was mainly located in the cytoplasm. The tumors with pulmonary metastasis from the puerarin treatment groups had significantly lighter colors of COX-2 positive cells and particles than those of the control group (Figure 5C). Therefore, COX-2 was one of the important pathways by which puerarin suppressed the *in vivo* pulmonary metastasis

of A549 cells.

#### Discussion

In this study, more cells in the puerarin treatment groups were arrested in the G0/G1 phase than the control group, but the proportion of S phase cells decreased. Thus, puerarin inhibited the proliferation of A549 cells by interfering with their cell cycle.

Tumor cells metastasize through at least two repeated processes of adhesion and invasion of the basement membrane (22). Tumor cells first bind laminin, fibronectin and collagen in the basement membrane and matrix through receptors on the membrane surface. Then they secrete or utilize various types of proteases (e.g., MMPs) to degrade the basement membrane and matrix. Finally, they directionally move and penetrate the broken basement membrane and matrix to complete invasion (23). In this study, after 24 h of culture with 200  $\mu\text{g/mL}$  puerarin,

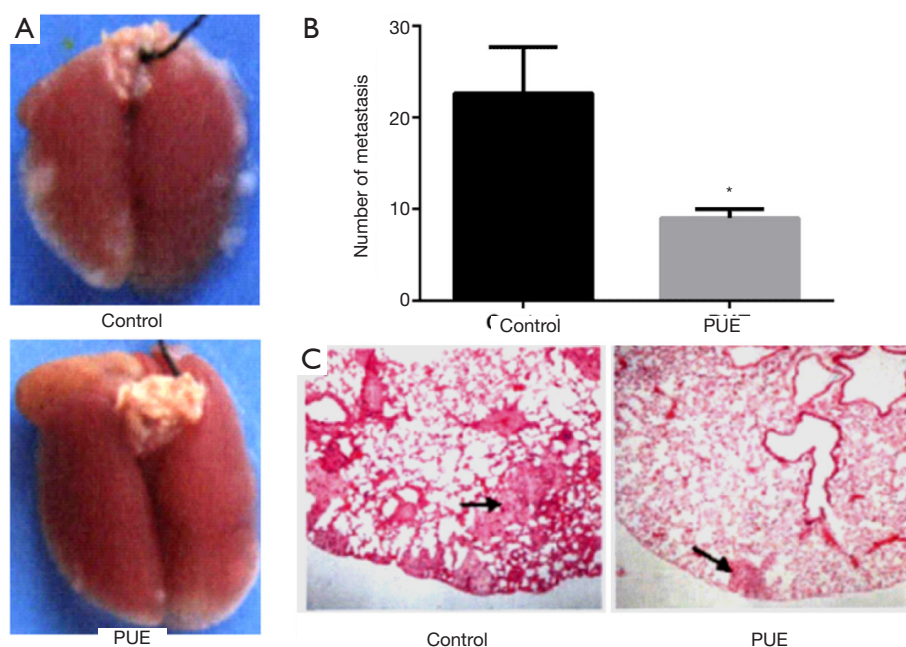


**Figure 4** Effects of puerarin on the distal metastasis of A549 cells. (A) A mouse model of lung metastasis was established by injection of A549 cells via the tail vein; (B) number of metastatic tumors after intraperitoneal injection of 100 mg/kg/day puerarin for 28 days; (C) HE staining results ( $\times 200$ ), arrows indicate tumors with pulmonary metastasis. \*,  $P < 0.05$ , compared with the control group.

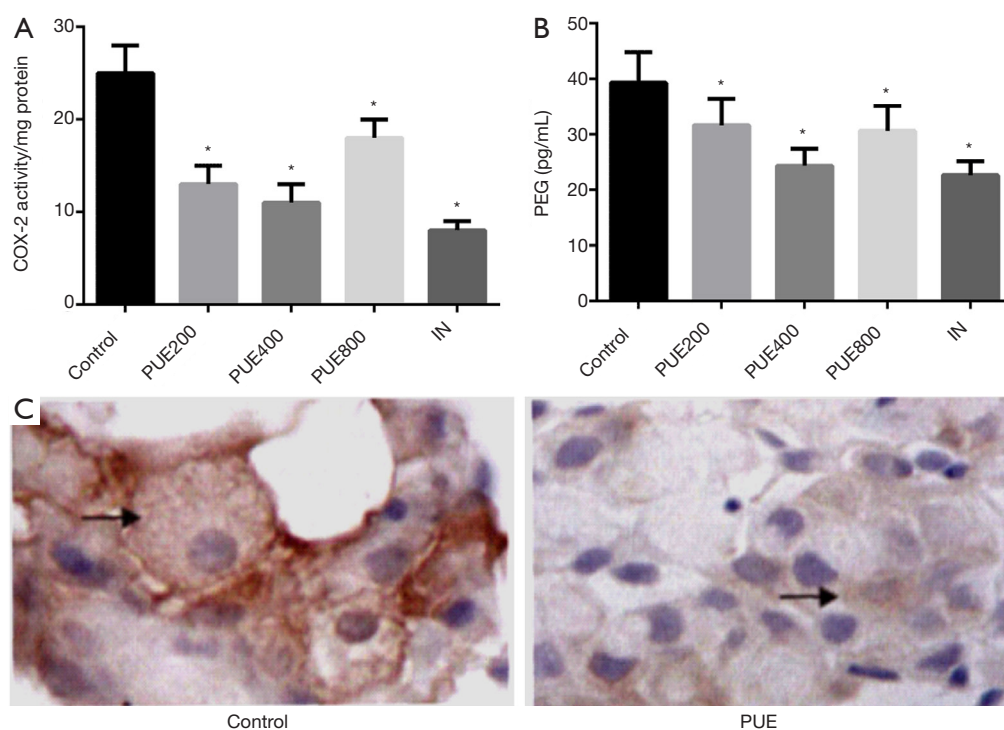


**Figure 5** Effects of puerarin on the enzymatic activity of COX-2 and PGE2. (A) Effects of different concentrations of puerarin on COX-2 enzymatic activity; (B) PGE2 levels in the supernatants of A549 cells after 24 h of puerarin treatment; (C) immunohistochemical assay results ( $\times 400$ ), arrows indicate COX-2 positive cells and particles. \*,  $P < 0.05$ , compared with the control group. COX-2, cyclooxygenase-2.

significantly fewer cells penetrated the basement membrane of Transwell chambers than those in the control group, verifying that puerarin significantly suppressed the invasion of A549 cells.

Tumor invasion is hallmarked by the degradation of extracellular matrix. Of the protein kinases promoting extracellular matrix degradation, MMPs play crucial roles in tumor invasion and metastasis, and MMP-2 is a key member of this family. MMP-2 has a corresponding tissue inhibitor TIMP-2 that binds the  $Zn^{2+}$  active site of MMP-2 according to a 1:1 ratio. It can also bind the zymogen form of MMP-2, thereby inhibiting its activity and maintaining a dynamic balance (24,25). Until now, the effects of puerarin on MMP-2 have never been reported. In this study, after 24 h of culture, the levels in PUE200, PUE400 and PUE800 groups significantly decreased compared those of the control group, further confirming that puerarin inhibited the invasion of A549 cells. On the other hand, we herein prompted for the first time that MMP-2/TIMP-2 may be one of the mechanisms by which puerarin suppressed their invasion.

Although the roles of puerarin in tumor invasion and metastasis remain controversial hitherto, we indeed found that it inhibited these processes of A549 cells. Compared with conventional chemotherapeutic agents with evident toxic side reactions, puerarin did not significantly alter the diet or body weight of mice, so it was safe for the prevention and treatment of lung cancer.

COX-2 participates in the growth, proliferation, invasion and metastasis of lung cancer, as an important molecular target in prevention and treatment (26). Puerarin inhibited the enzymatic activity of COX-2 and PGE2 generation in A549 cells in this study, and less COX-2 was expressed in puerarin treatment groups than in the control group. Hence, the COX-2 pathway was one of the mechanisms by which puerarin exerted antitumor effects. Notably, *in vitro* experiments showed that puerarin hardly affected COX-2 protein expression in A549 cells, but *in vivo* experiments displayed that COX-2 expression in the mice bearing tumors with pulmonary metastasis significantly decreased. Accordingly, puerarin may affect COX-2 expression also via other pathways.

## Conclusions

In summary, puerarin significantly attenuated the invasion ability of A549 cells, and reduced the levels of COX-2 and MMP-2/TIMP-2 compared with those of the control

group, indicating that the inhibitory effects of puerarin were closely associated with its resistance to tumor invasion. Nevertheless, whether puerarin suppresses MMP-2/TIMP-2 directly or via the COX-2 pathway still needs in-depth studies.

## Acknowledgments

*Funding:* None.

## Footnote

*Conflicts of Interest:* All authors have completed the ICMJE uniform disclosure form (available at <http://dx.doi.org/10.21037/tcr.2017.06.18>). The authors have no conflicts of interest to declare.

*Ethical Statement:* The authors are accountable for all aspects of the work in ensuring that questions related to the accuracy or integrity of any part of the work are appropriately investigated and resolved. The study was conducted in accordance with the Declaration of Helsinki (as revised in 2013). Institutional ethical approval and informed consent were waived. All experiments were performed in accordance with the guidelines for the care and use of laboratory animals and related ethical regulations of Jiangsu Cancer Hospital (No. 20160036).

*Open Access Statement:* This is an Open Access article distributed in accordance with the Creative Commons Attribution-NonCommercial-NoDerivs 4.0 International License (CC BY-NC-ND 4.0), which permits the non-commercial replication and distribution of the article with the strict proviso that no changes or edits are made and the original work is properly cited (including links to both the formal publication through the relevant DOI and the license). See: <https://creativecommons.org/licenses/by-nc-nd/4.0/>.

## References

1. Levy BP, Rao P, Becker DJ, et al. Attacking a Moving Target: Understanding Resistance and Managing Progression in EGFR-Positive Lung Cancer Patients Treated with Tyrosine Kinase Inhibitors. *Oncology* (Williston Park) 2016;30:601-12.
2. Hiley CT, Le Quesne J, Santis G, et al. Challenges in molecular testing in non-small-cell lung cancer patients with advanced disease. *Lancet* 2016;388:1002-11.



3. Simon ST, Higginson IJ, Booth S, et al. Benzodiazepines for the relief of breathlessness in advanced malignant and non-malignant diseases in adults. *Cochrane Database Syst Rev* 2016;10:CD007354.
4. Redzović A, Dintinjana RD, Nacinovic AD. Indicators of Cellular and Developmental Disorders in Multiple Primary Cancers. *Coll Antropol* 2016;40:59-62.
5. Hirsch FR, Suda K, Wiens J, et al. New and emerging targeted treatments in advanced non-small-cell lung cancer. *Lancet* 2016;388:1012-24.
6. Manganelli R, Manganelli S, Iannaccone S, et al. Management of antirheumatic drugs in kidney failure. *G Ital Nefrol* 2015;32. pii: gin/32.6.4.
7. Papageorgiou N, Zacharia E, Briasoulis A, et al. Celecoxib for the treatment of atherosclerosis. *Expert Opin Investig Drugs* 2016;25:619-33.
8. Wang X, Huycke MM. Colorectal cancer: role of commensal bacteria and bystander effects. *Gut Microbes* 2015;6:370-6.
9. Luo D, Long Y, Chen GJ. Cyclooxygenase-2 gene polymorphisms and risk of Alzheimer's disease: A meta-analysis. *J Neurol Sci* 2015;359:100-5.
10. Echizen K, Hirose O, Maeda Y, et al. Inflammation in gastric cancer: Interplay of the COX-2/prostaglandin E2 and Toll-like receptor/MyD88 pathways. *Cancer Sci* 2016;107:391-7.
11. Kroon FP, van der Burg LR, Ramiro S, et al. Nonsteroidal Antiinflammatory Drugs for Axial Spondyloarthritis: A Cochrane Review. *J Rheumatol* 2016;43:607-17.
12. Stitham J, Hwa J. Prostacyclin, Atherothrombosis and Diabetes Mellitus: Physiologic and Clinical Considerations. *Curr Mol Med* 2016;16:328-42.
13. Paleari L, Puntoni M, Clavarezza M, et al. PIK3CA Mutation, Aspirin Use after Diagnosis and Survival of Colorectal Cancer. A Systematic Review and Meta-analysis of Epidemiological Studies. *Clin Oncol (R Coll Radiol)* 2016;28:317-26.
14. Langhendries JP, Allegaert K, Van Den Anker JN, et al. Possible effects of repeated exposure to ibuprofen and acetaminophen on the intestinal immune response in young infants. *Med Hypotheses* 2016;87:90-6.
15. Rotim Z, Bolanca Z, Rogulj AA, et al. Oral lichen planus and oral lichenoid reaction--an update. *Acta Clin Croat* 2015;54:516-20.
16. Tang YH, Zhu HQ, Zhang YC, et al. Apoptosis of NB4 cells induced by flavonoids of puerarin in vitro. *Zhongguo Shi Yan Xue Ye Xue Za Zhi* 2010;18:326-9.
17. Shao HM, Tang YH, Jiang PJ, et al. Inhibitory effect of flavonoids of puerarin on proliferation of different human acute myeloid leukemia cell lines in vitro. *Zhongguo Shi Yan Xue Ye Xue Za Zhi* 2010;18:296-9.
18. Ji O, Shen Q, Si YJ. Effect of flavonoids of puerarin on the proliferation and apoptosis of retinoic acid resistant acute promyelocytic leukemia cell line NB4-R1 cells. *Zhonghua Xue Ye Xue Za Zhi* 2013;34:455-7.
19. Huang H, Al-Shabrawey M, Wang MH. Cyclooxygenase- and cytochrome P450-derived eicosanoids in stroke. *Prostaglandins Other Lipid Mediat* 2016;122:45-53.
20. Marshall J. Transwell® invasion assays. *Methods Mol Biol* 2011;769:97-110.
21. Li W, Tian H, Li L, et al. Diallyl trisulfide induces apoptosis and inhibits proliferation of A549 cells in vitro and in vivo. *Acta Biochim Biophys Sin (Shanghai)* 2012;44:577-83.
22. Oliveira C, Ribeiro AJ, Veiga F, et al. Recent Advances in Nucleic Acid-Based Delivery: From Bench to Clinical Trials in Genetic Diseases. *J Biomed Nanotechnol* 2016;12:841-62.
23. Dunga JA, Adamu Y, Kida IM, et al. Tobacco abuse and its health effect. *Niger J Med* 2015;24:354-62.
24. Zumla A, Rao M, Dodoo E, et al. Potential of immunomodulatory agents as adjunct host-directed therapies for multidrug-resistant tuberculosis. *BMC Med* 2016;14:89.
25. Burdett S, Rydzewska L, Tierney J, et al. Postoperative radiotherapy for non-small cell lung cancer. *Cochrane Database Syst Rev* 2016;10:CD002142.
26. Zargaran A, Borhani-Haghighi A, Faridi P, et al. A review on the management of migraine in the Avicenna's Canon of Medicine. *Neurol Sci* 2016;37:471-8.

**Cite this article as:** Zeng Y, Shen ZJ, Gu WZ, Wu MH. Cyclooxygenase-2 mediates puerarin to inhibit the invasion and metastasis of lung cancer A549 cells. *Transl Cancer Res* 2017;6(3):493-501. doi: 10.21037/tcr.2017.06.18